Supporting Information

Influence of Zn^{2+} and S^{2-} on the Formation of $CsPbBr_3$ Nanocrystals in Fluorophosphate Glass

Kejie Huang,[a] Ruilin Zheng,*[abc] Seiya Shimono,[d] Kenji Shinozaki,[e] Takayuki Nakanishi,[f] Jian Xu,*[ag] and Setsuhisa Tanabe[ag]

a. Graduate School of Human and Environmental Studies, Kyoto University, Kyoto, Kyoto 606-8316, Japan

b. College of Science, Nanjing University of Posts and Telecommunications, Nanjing, Jiangsu 210023, China

c. Advanced Laser and Optoelectronic Functional Materials Department, Shanghai Institute of Optics and Fine Mechanics, Chinese Academy of Science, Shanghai, 201800, China.

d. Diffraction and Scattering Division, Japan Synchrotron Radiation Research Institute, Sayo, hyogo 679-5198, Japan

e. Research Institute of Core Technology for Materials Innovation, National Institute of Advanced Industrial Science and Technology (AIST), Ikeda, Osaka 563-8577, Japan

f. Advanced Phosphor Group, National Institute for Materials Science (NIMS), Tsukuba, Ibaraki 305-0044, Japan

g. Graduate School of Global Environmental Studies (GSGES), Kyoto University, Kyoto, Kyoto 606-8501, Japan

Corresponding e-mail addresses:

ruilinzheng@hotmail.com

xu.jian.3z@kyoto-u.ac.jp

Experimental section

Fabrication of $CsPbBr_3$-embedded fluorophosphate glass-ceramics

The conventional melt-quench method was applied for the fabrication of glass samples ($48NaPO_3$-$20Al(PO_3)_3$-10NaF-$17SrF_2$-2CsBr-$2PbBr_2$-SrF_2/ZnO/SrS). Sodium metaphosphate ($NaPO_3$, 99.99%), aluminum metaphosphate ($Al(PO_3)_3$, 99.99%) and sodium fluoride (NaF, 99.99%) were purchased from TaiYang Technology Co., Ltd. Cesium bromide (CsBr, 99.0%) was purchased from Tokyo Chemical Industry. Strontium fluoride (SrF_2, 99.0%) and zinc oxide (ZnO, 99.999%) were purchased from Furuuchi Chemical. Strontium sulfide (SrS, 99.9%) was purchased from Strem Chemicals. For reference sample, 6.99 g $NaPO_3$, 7.53 g $Al(PO_3)_3$, 0.60 g NaF, 3.23 g SrF_2, 1.05 g $PbBr_2$, 0.61 g CsBr were mixed and transferred to a furnace preheated to 900°C for 20 minutes. The melted glass was quenched onto a room-temperature stainless-steel plate. The obtained as-made glass sample was transferred to another furnace preheated to 300 °C, annealing for 2 h to release the thermal strain. The sample was cut and double-face polished for measurements. For the +Zn sample, the raw material consisted of 7.01 g $NaPO_3$, 7.56 g $Al(PO_3)_3$, 0.60 g NaF, 3.06 g SrF_2, 1.05 g $PbBr_2$, 0.61 g CsBr and 0.12 g ZnO. For the +S sample, the raw material consisted of 6.99 g $NaPO_3$, 7.54 g $Al(PO_3)_3$, 0.60 g NaF, 3.05 g SrF_2, 1.05 g $PbBr_2$, 0.61 g CsBr and 0.17 g SrS.

Sample preparation for spectral measurement

After the fabrication of bulk as-made sample, the sample was first cut into pieces. Some pieces were polished for *in-situ* transmittance measurements. A 2-hour heat treatment at 360 °C was applied to the rest of the sample. The heat-treated pieces were ground into powders. The powder was used for the total scattering spectrum and XRD measurements. For temperature-dependent PL spectroscopy, glass powder was mixed with boron nitride (BN) in 1:1 weight ratio to avoid self-absorption.

Characterization of the reference, +Zn and +S samples

Differential scanning calorimetry (DSC) measurements were performed on a Rigaku ThermoPlus DSC 8230 at a heating rate of 10 °C/min in air. Standard Al_2O_3 powder was used as a reference. Glass powder before heat treatment was used as the target sample. The optical

transmittance spectra were measured by a CCD spectrometer (QE65Pro, Ocean Optics) with a Xenon lamp (MAX-302, Asahi-Spectra). The sample was set on a thermal stage (10033L, Linkam) for temperature control. The optical bandgap was determined by the *Tauc* plot method. High-energy X-ray scattering in transmission geometry was performed at the beamline BL04B2 of SPring-8, Japan. Synthetic samples were filled into a borosilicate glass capillary with a diameter of 2 mm. The wavelength of the incident X-rays was monochromatized to 112.8 keV, and the high-energy X-ray scattering patterns were collected using two-dimensional LAMBDA 750K CdTe detector. The pair distribution function (PDF) was calculated using the Orochi software [1]. The powder X-ray diffraction (XRD) pattern was recorded by an X-ray diffractometer (SmartLab X-ray Diffractometer, Rigaku) with Cu-$K_{\alpha 1}$ radiation at 45 kV, 200 mA, and 2θ in the range of 5–80°. The MCPD-9800 spectrometer, in combination with an integrating sphere, was also used to measure the internal quantum efficiency (IQE). The temperature-dependent photoluminescence (PL) spectra were measured by a CCD spectrometer (QE65Pro, Ocean Optics) with a 365 nm LED lamp (LED365－SPT/L, OptoCode). The sample was set on a thermal stage (10033L, Linkam) for temperature control. All transmittance spectra were normalized to the transmittance at 590 nm of the sample prior to heat treatment, in order to minimize baseline variations caused by the Linkam stage.

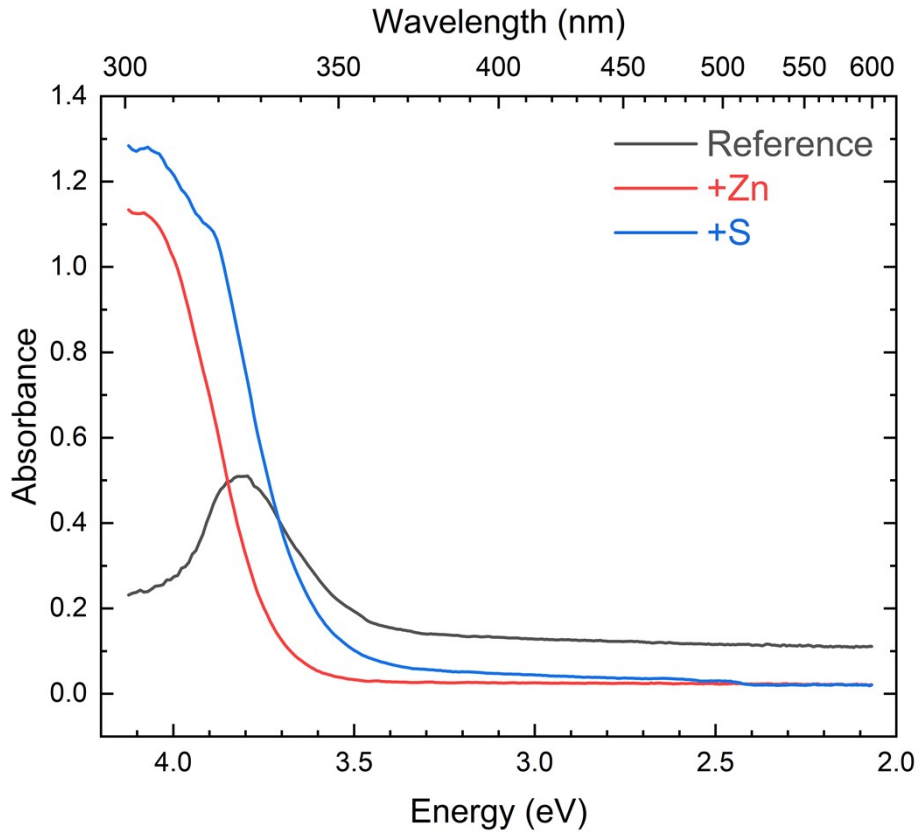

Fig. S1. Absorbance spectra of the as-made reference, +Zn and +S samples.

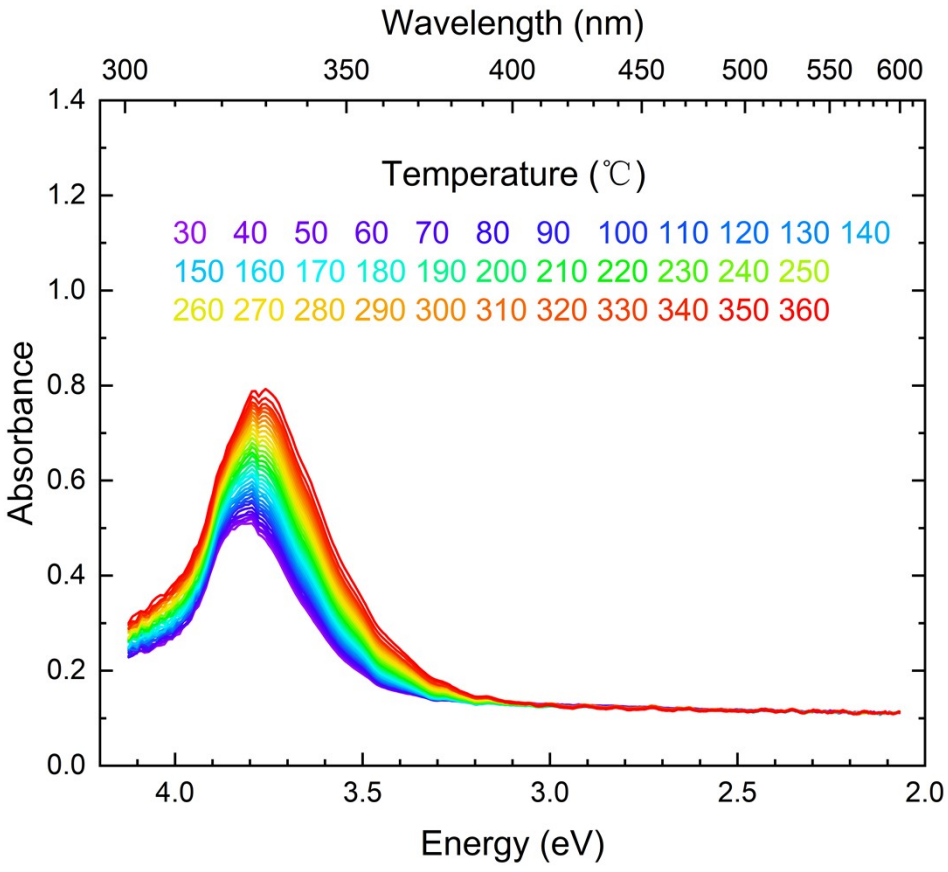

Fig. S2. Absorbance spectra of the reference sample during the heating stage.

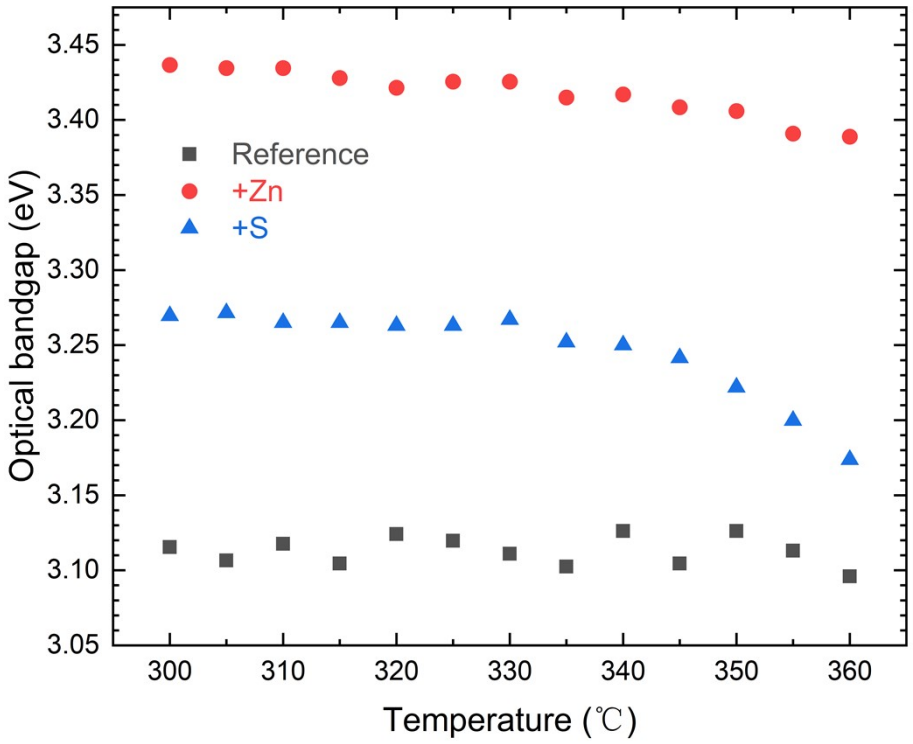

Fig. S3. Optical bandgap evolution during 300-360℃; Bandgap energy calculated with indirect allowed transitions.

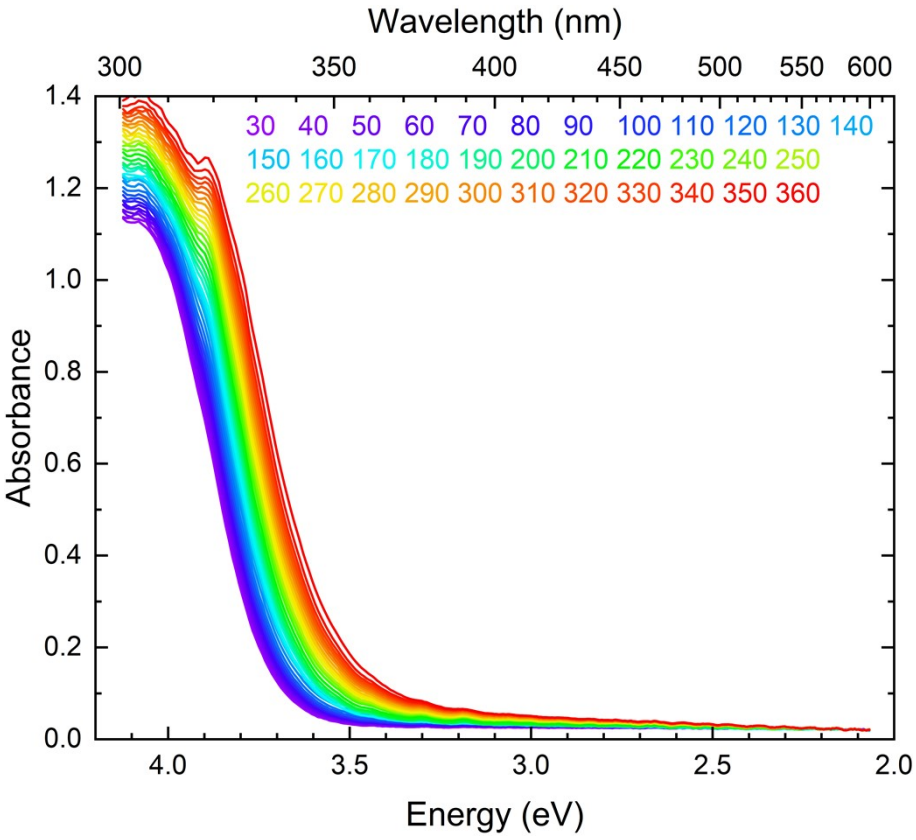

Fig. S4. Absorbance spectra of the +Zn sample during the heating stage.

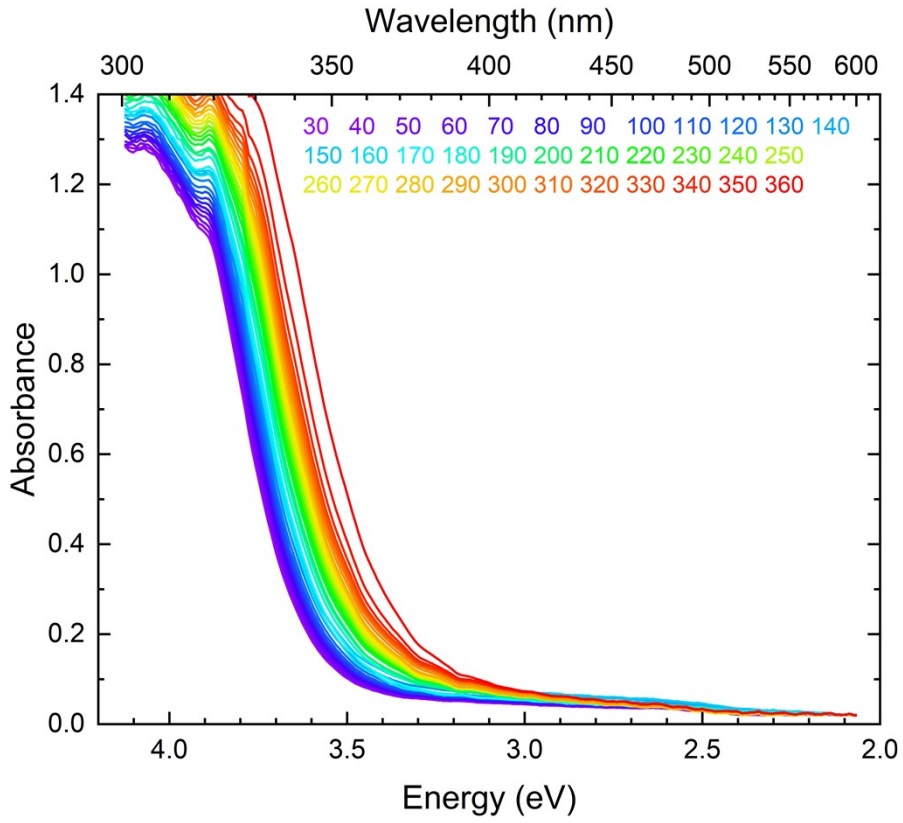

Fig. S5. Absorbance spectra of the +S sample during the heating stage.

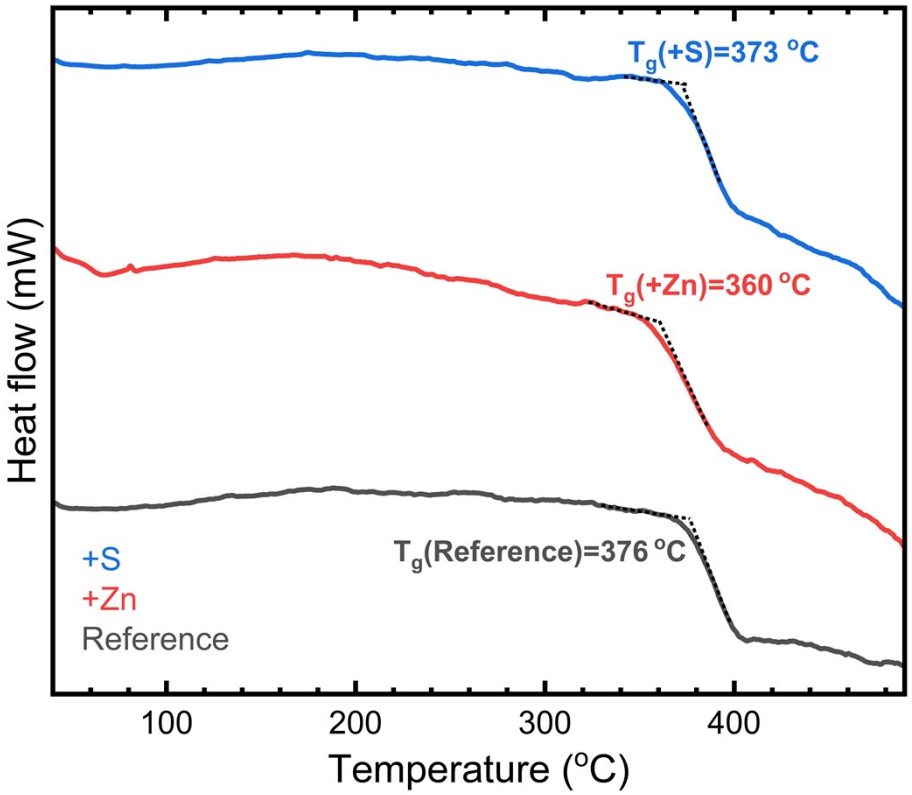

Fig. S6. Differential Scanning Calorimetry (DSC) curve of the reference/+Zn/+S sample (the heating rate was 10℃/min; T_g was determined using the onset method).

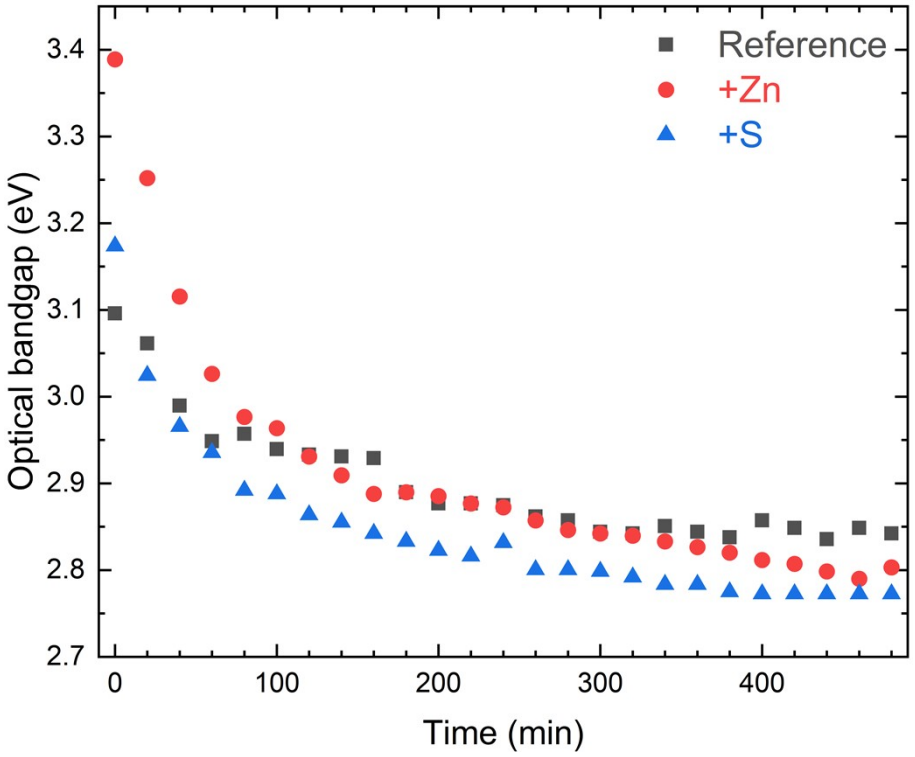

Fig. S7. Optical bandgap evolution of the samples during the holding stage (0~480 min); Bandgap energy calculated with indirect allowed transitions.

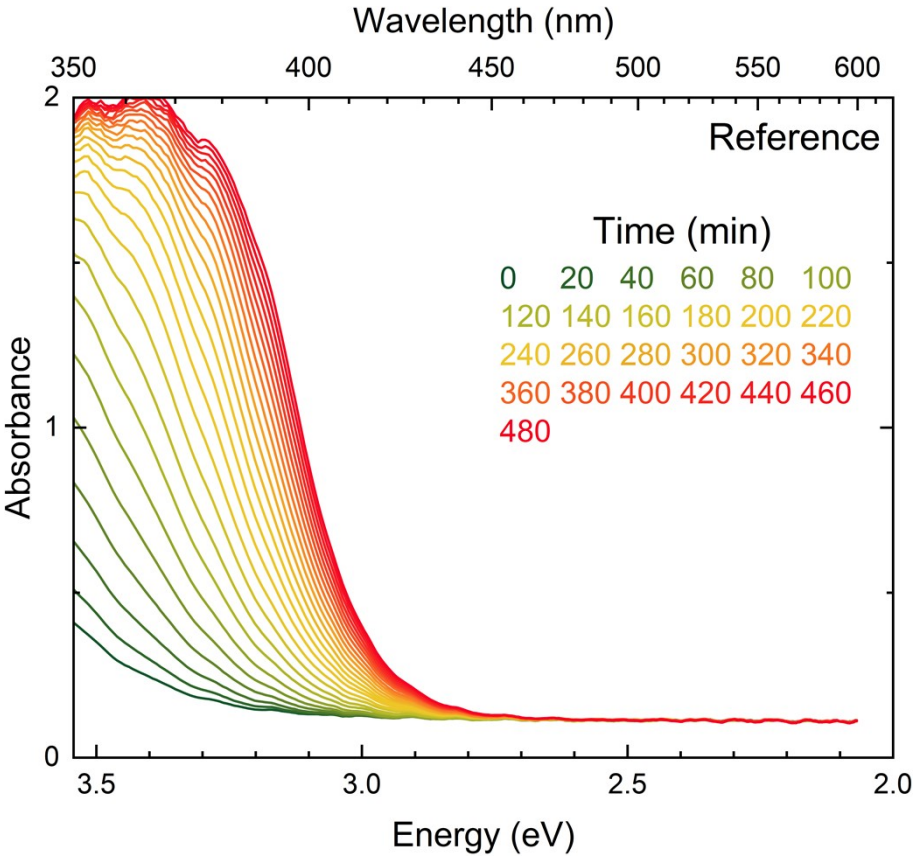

Fig. S8. Absorbance spectra of the reference sample during the holding stage.

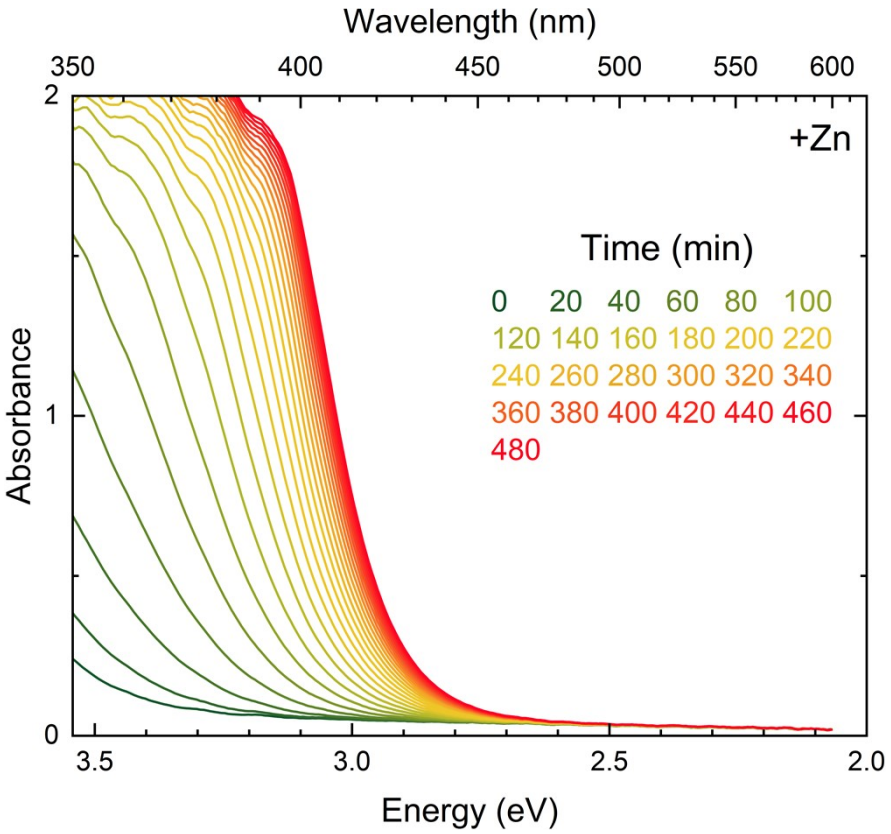

Fig. S9. Absorbance spectra of the +Zn sample during the holding stage.

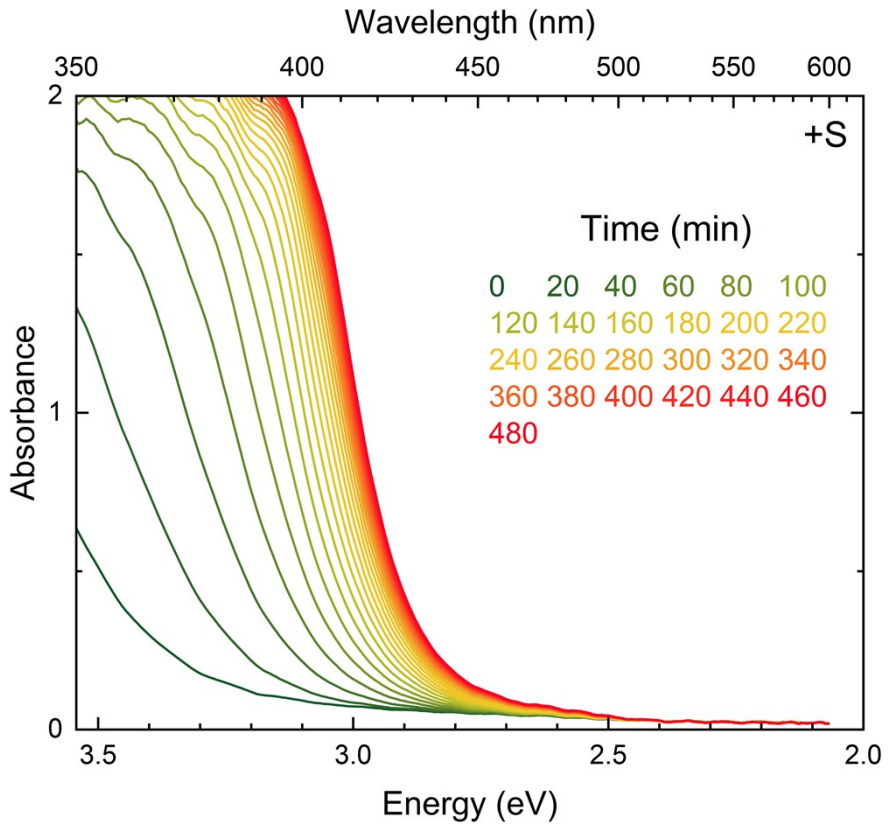

Fig. S10. Absorbance spectra of the +S sample during the holding stage.

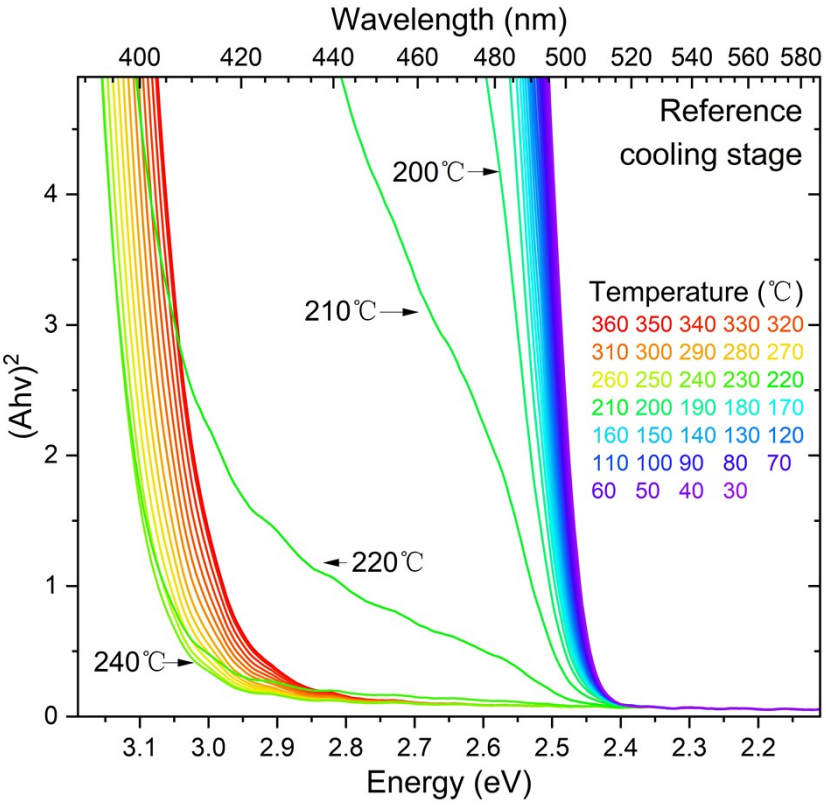

Fig. S11. *Tauc* plot of absorbance evolution of the reference sample during cooling stage.

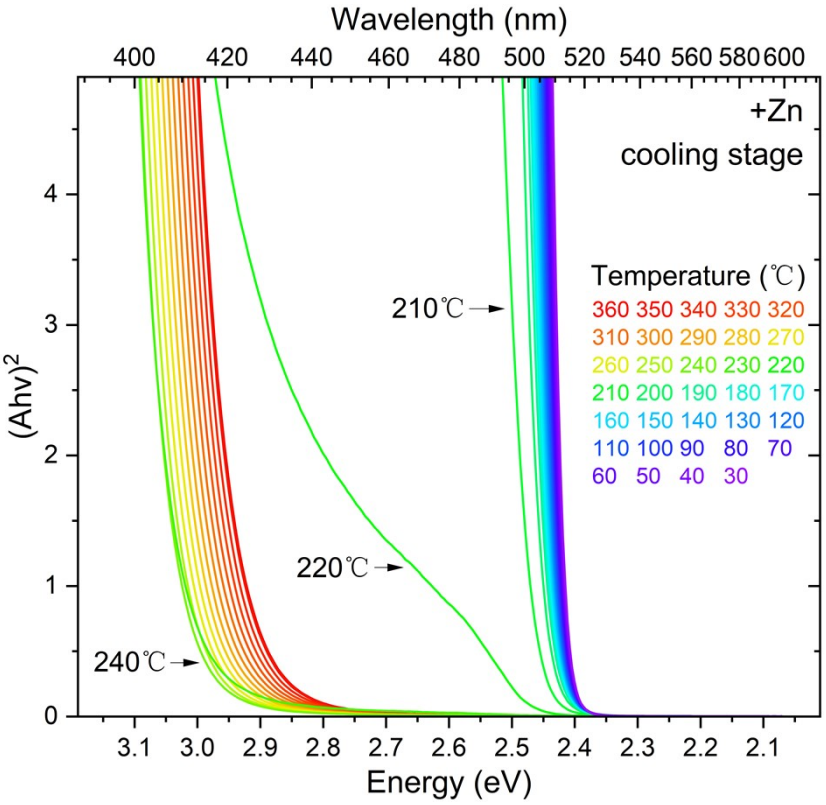

Fig. S12. *Tauc* plot of absorbance evolution of the +Zn sample during cooling stage.

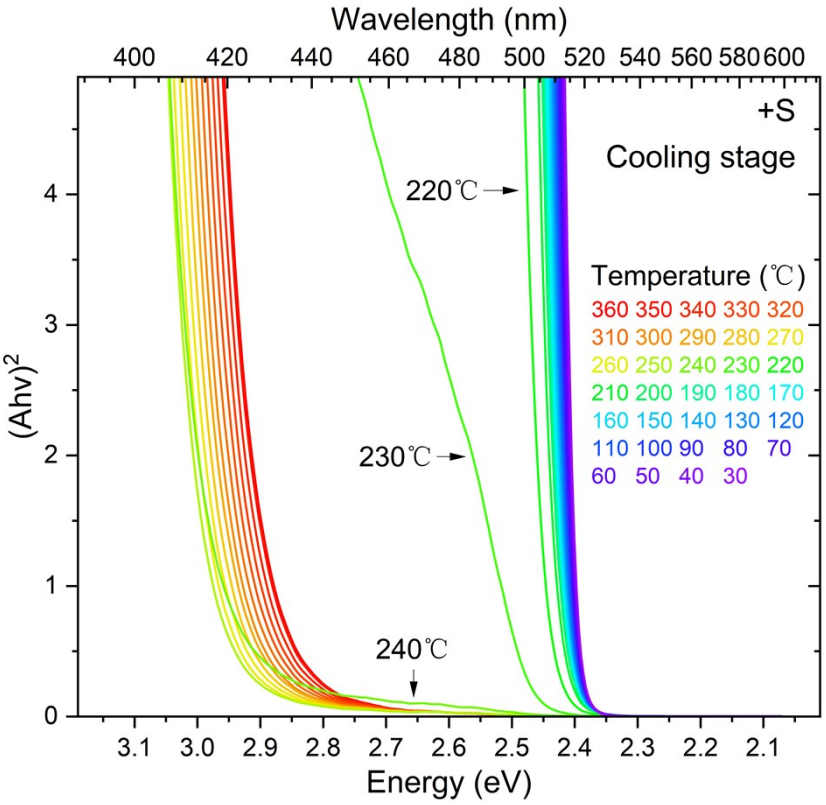

Fig. S13. *Tauc* plot of absorbance evolution of the +S sample during cooling stage.

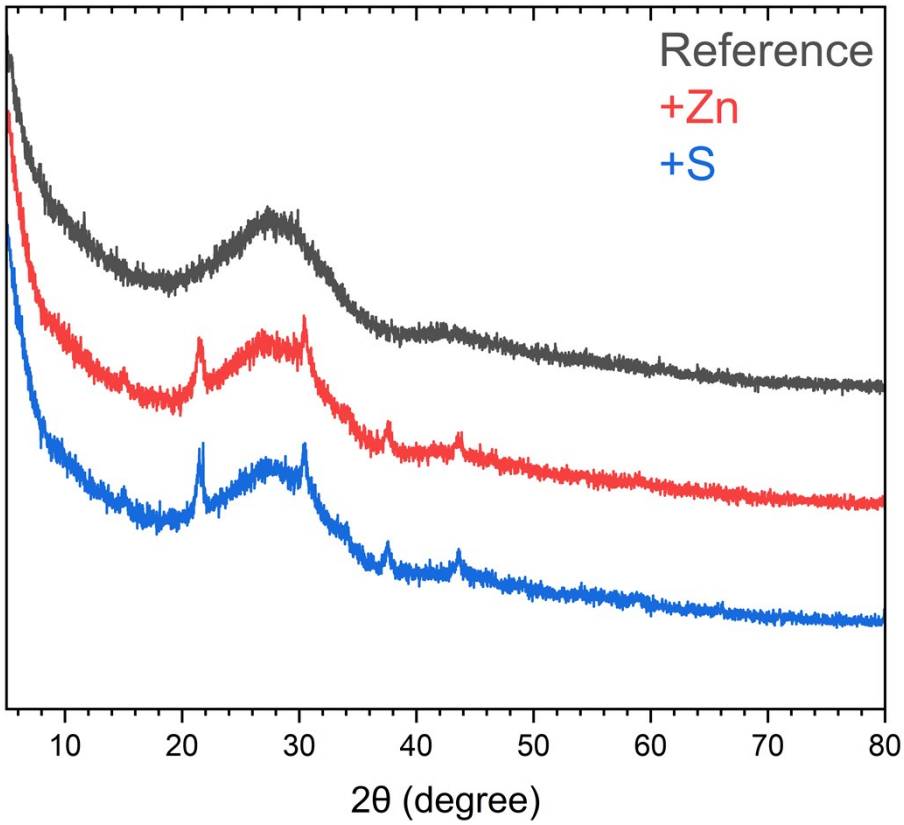

Fig. S14. XRD patterns of the reference, +Zn and +S samples.

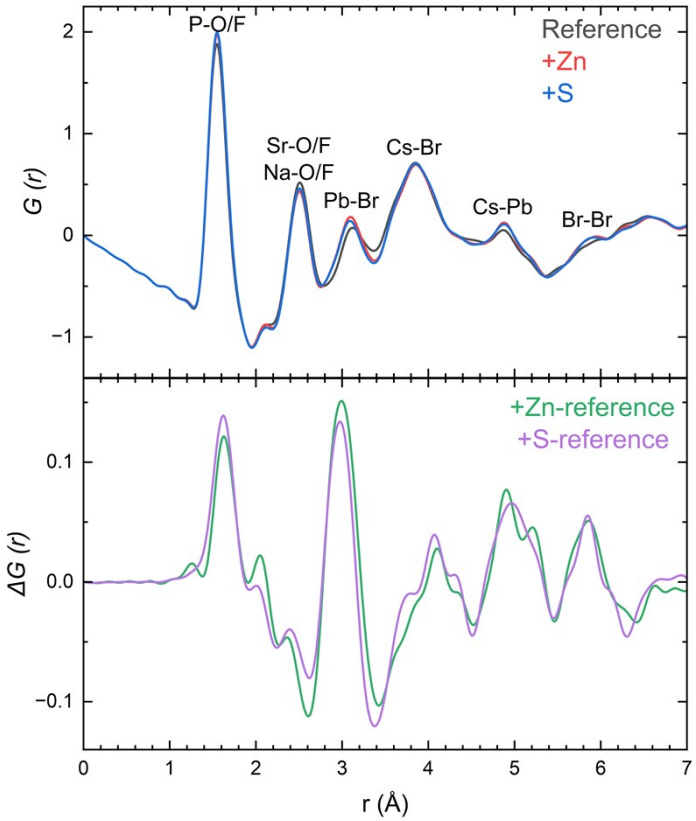

Fig. S15. *G(r)* profile and Difference pair distribution function (d-PDF) of the reference, +Zn and +S samples.

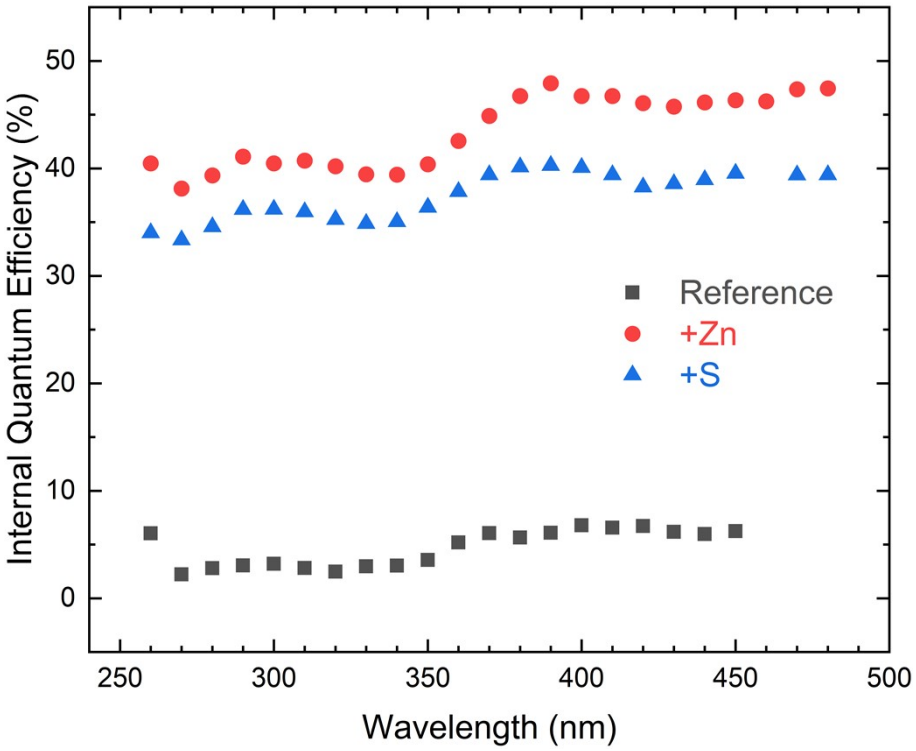

Fig. S16. Excitation wavelength dependence of internal quantum efficiency (IQE) of the reference, +Zn and +S samples.

Reference

[1] S. Tominaka, H. Yamada, S. Hiroi, S. I. Kawaguchi, K. Ohara, *ACS Omega*, 2018, **3**, 8874-8881.

Author contribution statement

K. H. participated in the sample preparation, data collection, data analysis, writing original draft; R. Z. participated in the data collection, data analysis, writing review & editing; S. S. and K. S. participated in the X-ray total scattering data collection and PDF analysis; T. N. participated in the PL and XRD data collection and analysis; J. X. participated in data collection, data analysis, writing review & editing; S. T. participated in writing review & editing.